NEW AB INITIO POTENTIAL CURVE AND QUASIBOUND STATES OF HeH+ *

W. KOŁOS

Max-Planck-Institute for Physics and Astrophysics, 8 Munich 40, Federal Republic of Germany and Quantum Chemistry Laboratory, University of Warsaw, 02-093 Warsaw, Poland **

and

J.M. PEEK

Sandia Laboratories, Albuquerque, New Mexico 87115, USA

The ground state energy of HeH+ has been calculated in the Born–Oppenheimer approximation for $0.9 \leqslant R \leqslant 4.5$ au by using an 83-term variational wavefunction in elliptic coordinates and including the interelectronic distance. The resulting potential curve has been used to compute the quasibound state spectrum of the ion.

1. Introduction

Experimental measurements [1–3] of the proton production cross section from isotopes of HeH+ have stimulated theoretical work [4–5] on the quasibound states of the ion. The observed resonances have been identified, and since the theoretical and experimental energies were not in satisfactory agreement it seemed natural to attribute the discrepancy to an insufficiently accurate potential curve for the electronic ground state of HeH+. To clarify this point a more accurate potential has been computed for a wide range of internuclear distances in HeH+ and the results are reported in section 2 of the present paper, where the correlation energy of the ion is also presented. Section 3 contains the energies and widths of all quasibound states of ^{3}HeH+ and ^{4}HeH+ obtained with the new potential, their discussion and comparison with the experimental data.

2. Potential energy curve

One of the present authors has already calculated [6] the potential energy curve for the ground state of HeH+ for internuclear distances $5 \leqslant R \leqslant 9$ au. The wavefunction was assumed to be in the form of an expansion in elliptic coordinates and depended explicitly on the interelectronic distance. Using the same wavefunction we have extended the calculation to $0.9 \leqslant R \leqslant 4.5$ au. The 83 terms of the wavefunction used in the final computation had been selected in numerous test runs made at $R = 1.46$, 3.0 and 6.0 au. The exponents in the wavefunction were optimized in a 45-term expansion at $R = 0.9$, 1.46, 1.8, 3.0, 4.5, 6.0 and these values were used in the final runs with the 83-term wavefunction. For intermediate internuclear distances the exponents were interpolated. Only the β_2 exponent was optimized for some additional R values. The results of the computation are shown in table 1 where in addition to the total energy, E, we list the binding energy, D, and the derivative dE/dR obtained from the virial theorem.

For $1.1 \leqslant R \leqslant 1.8$ au the present results overlap with those of Wolniewicz [7] obtained using a 64-term wavefunction of the same form. In this region our total energies are 7–9 cm^{-1} lower than his values. It is difficult to assess the accuracy of the present results. However,

Table 1
Energies of HeH$^+$ in the X$^1\Sigma^+$ state calculated in the Born-Oppenheimer approximation using an 83-term wavefunction [a]

R	E	D [b]	dE/dR
0.9	−2.84562504	−12748.90	−0.74384593
1.0	−2.90478633	235.50	−0.45989130
1.1	−2.94091999	8165.92	−0.27566525
1.2	−2.96203002	12799.04	−0.15481689
·1.3	−2.97326109	15263.97	−0.07524032
1.4	−2.9779945S	16302.84	−0.02304952
1.46	−2.97868906	16455.27	−0.00101162
1.4631	−2.97869074	16455.64	−0.00002487
1.4632	−2.97869074	16455.64	0.00000678
1.4633	−2.97869074	16455.64	0.00003842
1.5	−2.97848894	16411.35	0.01071387
1.6	−2.97627233	15924.86	0.03195637
1.7	−2.97238658	15072.04	0.04463694
1.8	−2.96754491	14009.41	0.05145261
1.9	−2.96223694	12844.45	0.05425191
2.0	−2.95679360	11649.77	0.05433991
2.2	−2.94631420	9349.81	0.04977668
2.4	−2.93708703	7324.68	0.04235013
2.6	−2.92942701	5643.50	0.03438358
2.8	−2.92331226	4301.47	0.02701885
3.0	−2.91856551	3259.68	0.02074083
3.2	−2.91495455	2467.16	0.01565559
3.4	−2.91224263	1871.97	0.01169218
3.5	−2.91115754	1633.82	0.01008028
3.6	−2.91022210	1428.51	0.00868343
3.8	−2.90872167	1099.21	0.00644081
4.0	−2.90760688	854.54	0.00478957
4.5	−2.90589760	479.39	0.00234968

[a] All results in atomic units, only D in cm^{-1}.
[b] Relative to the energy of the helium atom E = −2.90371332 au obtained with the same wavefunction [6].

since the same wavefunction applied to the helium atom [6] gives an energy which is about 2 cm^{-1} higher than the exact value, it is likely that for HeH$^+$ the error is roughly of the same order of magnitude.

Using the present results and the SCF energies computed by Peyerimhoff [8] one gets the correlation energy of the HeH$^+$ ion listed in table 2 for several internuclear separations. The correlation energy is also shown graphically in fig. 1 where the present results are supplemented with the asymptotic correlation energies [6].

Table 2
Correlation energy of HeH$^+$ (in au)

R	E_{corr}	R	E_{corr}
1.0	0.04375	2.0	0.04559
1.2	0.04464	2.2	0.04511
1.3	0.04506	2.8	0.04353
1.4	0.04540	3.5	0.04254
1.5	0.04566	4.0	0.04227
1.6	0.04582	4.5	0.04215
1.7	0.04589	∞	0.04203
1.8	0.04586		

The latter were obtained from the multipole expansion of the interaction energy valid in the region where the overlap is negligible. The curve in fig. 1 shows how an approaching proton affects the correlation energy of the helium atom. The most characteristic feature of the above correlation energy is a minimum at large R and a very pronounced maximum in the vicinity of the equilibrium internuclear distance. At large R the electron correlation decreases the van der Waals attraction between He and H$^+$ which is understandable since the correlation decreases the induced dipole moment of the helium atom. However, at smaller R the correlation energy increases. Thus the SCF method seems to describe better an atom than a two-center molecular sys-
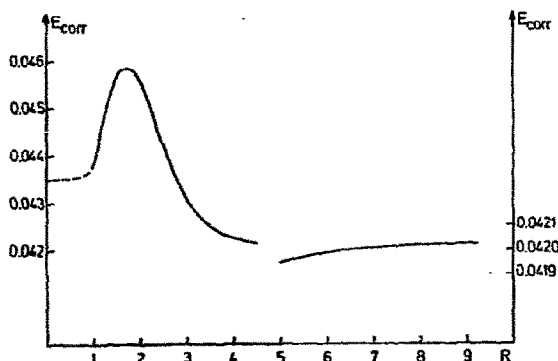

Fig. 1. Correlation energy of HeH$^+$ as function of the internuclear distance. The right hand side has been obtained as $E_{corr} = E_{corr}(R = \infty) + \Delta E_{corr}$, where ΔE_{corr} represents the difference of the induction energies calculated with and without electron correlation using the multipole expansion [6]. Note the change of scale.

tem. The maximum change of the helium atom corre-
lation energy due to the interaction with the proton
amounts to 9%.

3. Quasibound states

The availability of the improved data for the ground
state of HeH$^+$, presented in the previous Section, makes
it possible to remove a serious question concerned with
the location of certain quasibound rotation-vibration
(QB) states in this potential. A remarkable series of ex-
periments [1–3] succeeded in measuring dissociation
fragments from certain HeH$^+$ isotopes which have these
QB states as their origin. The energy of the resulting
fragments defines the energy above the dissociation
limit, ϵ, to an accuracy comparable to that obtained in
optical spectroscopy and various experimental param-
eters restrict the range of lifetimes, τ, for these states
in the continuum. A theoretical study [4] of the QB
states for several isotopes of HeH$^+$ was reasonably suc-
cessful in characterizing the experimental spectrum.
Using the restraints imposed by the experiment upon
the acceptable range of τ, rotation–vibration indices
were assigned to all but one observed state for ^{4}HeH$^+$
and ^{3}HeH$^+$ and all states predicted to be observable
were indeed observed for these cases. The deuterium
containing isotopes were more difficult to study experi-
mentally and the theoretically predicted spectrum did
not correlate as well with experiment for these cases
[4]. The theoretical predictions used a ground state
HeH$^+$ potential constructed from the best information
available at that time [9]. As the energies of the as-
signed states were, almost without exception, higher
than those observed, it was stated that this potential
could be as much as +0.001 hartree higher than the
true potential if the differences were due to errors in
the potential. Subsequently, by using a selected number
of these assignments and ignoring the lifetime restric-
tions, the experimental energies were shown to be ac-
curately represented by standard spectroscopic formu-
lae [5]. It was concluded that some single potential
would better represent the various isotopic spectra al-
though a corrected potential was not suggested [5].

The X$^1\Sigma^+$ HeH$^+$ potential presented in section 2 is
sufficiently accurate to remove any questions concern-
ing the predicted properties of the quasibound states.
Both the energies and widths resulting from this poten-

tial should not have errors which exceed those of the
experimental study. These data, presented below, will
resolve the question about the remaining differences
between experiment and theory, while satisfying the
requirement that a single adiabatic potential correctly
predicts the spectral for all HeH$^+$ isotopic species.

The QB spectra for ^{4}HeH$^+$ and ^{3}HeH$^+$ have been
recalculated using the a priori ground state potential
function presented here. The techniques used in this
calculation were substantially those described in ref.
[4]. The Born–Oppenheimer equation for nuclear mo-
tion

$$\Psi''(R, \epsilon) + p(R, \epsilon)\Psi(R, \epsilon) = 0, \tag{1}$$

where

$$p(R,\epsilon) = (2\mu/\hbar^2)[\epsilon - V(R)] - J(J + 1)R^{-2},$$

was solved by standard numerical techniques subject to
the conditions

$$\Psi(0,\epsilon) = 0 \tag{2}$$

and

$$\Psi'(\rho_3,\epsilon)/\Psi(\rho_3,\epsilon) \approx -0.72901\,[p'(\rho_3,\epsilon)]^{1/3}. \tag{3}$$

Here, μ is the reduced mass (the proton to electron mass
ratio was taken as 1836.109), ϵ is the energy of QB state
above the dissociation limit, J is the rotational quantum
number, and R is the internuclear separation. Primes in-
dicate derivatives with respect to R evaluated at the as-
signed value of the independent variable. The potential
$V(R)$ is defined by a cubic spline fit to the X$^1\Sigma^+$ HeH$^+$
data given above and in ref. [6] along with an extension
to large R by the formula

$$V(R) = -[0.6898\,R^{-4} + 1.22015\,R^{-6} + 5.007\,R^{-8}].$$

The data from table 1 and ref. [6] were normalized to
this form by the addition of the He eigenenergy, see
footnote [b] of table 1. Eq. (10) of ref. 4 was used for
the definition of width Γ, which is related to τ by
$\tau\Gamma = \hbar$.

Eqs. (1)–(3) define an eigenvalue problem and eq.
(3) has a restricted applicability. A QB state will occur
only when $p(R)$ has three first order zeros if $V(R)$ has
the usual properties of a bonding molecular potential.
Assume ϵ and J are such that this requirement is satis-
fied, then $p(\rho_3,\epsilon) = 0$ defines ρ_3, where ρ_3 is the largest
value of R for which $p(R,\epsilon)$ is zero. It is presumed that
an appropriate boundary condition on Ψ will provide

a good approximation to ϵ as found from the usual Breit–Wigner parameterization of the scattering phase shift [4]. The condition used here is stated by eq. (3). It is based on the Langer uniform asymptotic approximations to the two independent solutions of eq. (1) in the neighborhood $R \approx \rho_3$. The desired behavior of Ψ for R slightly less than ρ_3 is assumed [4] to be best described by the solution that increases as R decreases for $R \leqslant \rho_3$. (Also note that in this region $p'(R, \epsilon) > 0$.) The right hand side of eq. (3) is then the logarithmic derivative of this choice of the two Langer approximations at $R = \rho_3$. A different condition, eq. (9a) of ref. [4], was used in the previous study of HeH+ QB states. Both conditions are known to give good predictions for the QB energies [4,10] with the use of eq. (3) being better than eq. (9a) of ref. 4 [11]. Eq. (3) fails when a second order zero of $p(R)$ occurs [11]. An important example of this problem occurs when ϵ approaches the maximum energy of the trapping barrier. Alternative techniques are preferred for this situation [4], although a satisfactory replacement for eq. (3) is known [11].

Preliminary to finding ϵ and Γ, it is usual practice to enumerate the number of discrete and quasibound RV states. Using the methods developed in ref. [4] to treat the QB part of the spectra, the potential presented here differs for the proton containing isotopes in only one case from the results found for the older $V(R)$ [4,9]. This difference occurs for the $J = 7$ and vibrational index $v = 8$, (8,7), in the ^{3}HeH+ isotope case. The potential discussed in ref. [9] supports a bound state with this labeling while it is a quasibound state in the present potential. The similarity of the enumeration results reflects the small differences between these two potentials. The single difference implies the present potential is more repulsive than the potential used in the earlier work. This is indeed the case for $4.0\,a_0 \leqslant R \leqslant 6.0\,a_0$ and presumably this range of R is important enough to account for the promotion of the (8,7) discrete state into a QB state in the continuum.

In actuality, the enumeration procedures have been improved in one respect [11]. Some properties of the continuum with energies near the top of the trapping barrier were identified [4] as false resonances since the phase shift behavior was not easily described by the Breit–Wigner parameterization. This partitioning was admittedly somewhat arbitrary [4]. It has been possible to sharpen the definition of a QB state with the re-

sult that some states previously designated as false resonances now become QB states. The new definition does impose a mild restriction on $p(R)$ but it is an improvement in that, at least for the ^{4}HeH+ case, all resonance-like behavior which would predict an ϵ less than the maximum energy of the trapping barrier now is a QB state. If one uses the most inclusive definition of a false resonance discussed in ref. [4], most of any resonance-like behavior of the phase shift occurring for energies greater than that of the trapping barrier will now be associated with a false resonance.

An example of the preceding discussion is demonstrated in table 3, where the complete QB spectrum for ^{4}HeH+ is listed. The false resonances are indicated in table 3 as parenthetical entries. The energies are assumed to be equal to the maximum energy of the trapping barrier and, although their widths were not calculated, they can be expected to have widths as large or larger than a few percent of their energy. The (2,23) and (5,16) QB states shown in table 3 for the ^{4}HeH+ case were listed as false resonances in ref. [4]. This change in designation is due to the change in enumeration techniques [11] and not caused by differences in the two potentials. The appearance of false resonances in table 3 that were not included in table II of ref. [4] is a result of using the relaxed definition discussed above and again is not a result of the differences between the two potentials.

As discussed in ref. [4], the reclassification of the QB states and false resonances shown in table 3 is not unexpected and it demonstrates the correlation with the behavior of the phase shifts shown by fig. 2 of ref. [4] claimed in the preceding paragraph. Although the phase shift character was not recalculated for the new $X^1\Sigma^+$ potential, the general result must be quite like that shown in fig. 2 of ref. [4].

The QB spectrum for ^{3}HeH+, based on the enumeration scheme discussed in the preceding paragraphs, is also shown in table 3. The new QB state (8,7) is seen when these data are compared with table III of ref. [4]. The reason for this is discussed in a preceding paragraph. One false resonance shown in ref. [4] for this case (2,22), is now a QB state and four new false resonances are shown in table 3. These latter differences, again, are due to the changes in enumeration techniques.

The data shown in table 3 differ somewhat from those given in ref. [4]. These differences are demonstrated in table 4, where certain of the experimental data [1–3] are also listed. The ϵ from this work reflect the increased

Table 3

The complete quasibound spectra for $X^1\Sigma^+$ $^4HeH^+$ and $^3HeH^+$ are tabulated. The parenthetical entries are the false resonances discussed in the text. The energies, ϵ, and widths, Γ, are in Hartree units of energy. The symbols v and J are the usual vibration and rotation quantum numbers if one associates v with the number of radial nodes "trapped" inside the angular momentum barrier.

		$^4HeH^+$		$^3HeH^+$	
v	J	$\epsilon \times 10^3$	Γ	$\epsilon \times 10^3$	Γ
0	28	(15.86)			
0	27	12.7772	3.5−5		
1	25	10.0237	1.0−4		
2	23	7.7773	2.0−4		
3	21	(5.94)			
0	26	9.2097	8.2−8	12.3891	2.6−5
1	24	7.0185	2.8−7	9.6235	7.6−5
2	22	5.3053	8.3−7	7.3881	1.6−4
3	20	3.9948	2.9−6	(5.64)	
4	18	2.9984	1.3−5		
5	16	2.2225	6.1−5		
6	14	(1.54)			
0	25	5.3918	1.5−12	8.6786	4.1−8
1	23	3.7106	1.7−12	6.5040	1.3−7
2	21	2.5019	1.8−12	4.8332	3.9−7
3	19	1.6941	4.2−12	3.5853	1.5−6
4	17	1.2010	4.5−11	2.6615	8.1−6
5	15	0.9233	2.8−9	1.9542	4.7−5
6	13	0.7479	4.1−7	(1.34)	
7	11	0.5631	1.8−5		
0	24	1.4247	2.2−25	4.7179	2.2−13
1	22	0.2436	9.1−38	3.0834	1.3−13
2	20			1.9489	7.5−14
3	18			1.2346	1.1−13
4	16			0.8437	1.4−12
5	14			0.6638	2.7−10
6	12			0.5681	1.5−7
7	10			0.4357	1.3−5
8	8	0.0611	1.4−9	(0.235)	
9	6	0.0487	1.5−6		
10	4	(0.047)			
0	23			0.6083	5.7−33
8	7			0.0127	3.7−13
9	5			0.0210	2.9−7
10	3			(0.0007)	

Table 4

Theoretical ϵ and Γ data for the QB states predicted to be observable in the experimental background spectra of $^4HeH^+$ and $^3HeH^+$ are tabulated from ref. [4] and from this work. The corresponding experimental background spectra from ref. [3] are also shown

		ref. [4]		This work		Experiment [3]
v	J	$\epsilon \times 10^3$	Γ	$\epsilon \times 10^3$	Γ	$\epsilon \times 10^3$
0	25	5.4417	1.8−12	5.3918	1.5−12	4.96 ⎫
1	23	3.7813	2.5−12	3.7106	1.7−12	3.40 ⎪
2	21	2.5747	3.3−12	2.5019	1.8−12	2.31 ⎬ a)
3	19	1.7603	8.8−12	1.6941	4.2−12	1.52 ⎪
4	17	1.2511	9.2−11	1.2010	4.5−11	1.05 ⎭
						6.51 ⎫
0	24	4.7672	2.7−13	4.7179	2.2−13	4.60 ⎪
1	22	3.1534	2.2−13	3.0834	1.3−13	2.83 ⎪
2	20	2.0213	1.5−13	1.9489	7.5−14	1.79 ⎬ b)
3	18	1.2998	2.9−13	1.2346	1.1−13	1.15 ⎪
4	16	0.8909	4.2−12	0.8437	1.4−12	0.69 ⎭
5	14	0.6771	4.4−10	0.6638	2.7−10	

a) These data are for the $^4HeH^+$ isotope.
b) These data are for the $^3HeH^+$ isotope.

states satisfying the experimental constraints [3]. In fact, although the trends are in the correct direction, the comparison between experiment and theory is substantially identical to that presented in ref. [4]. For this reason further comparisons will not be presented.

As stated above, this new potential is too accurate to expect further refinements to produce changes of any magnitude in the QB spectra. Since Bernstein was able [5] to obtain a rather good fit to the experimental spectra by using spectroscopic formulae, an anomalous situation would seem to exist. However, a resolution appears to exist by drawing an analogy to the recent study of the mass spectrum of H_2 and its deuterium containing isotopes [12,13]. The H_2^+ quasibound spectrum is measured in this experiment [12] and the theoretically predicted [13] spectrum is based on a very accurate potential function. Differences not unlike those displayed in table 4 are found. However, if a theoretically predicted QB state is convoluted with a function that represents the experimental apparatus, the resulting feature appears at an energy in satisfactory agreement with experiment [12,13]. Although it is yet to be established, the differences between experiments and

bonding character of the potential for $R \leqslant 4.0\ a_0$ by being somewhat lower than the data presented in ref. [4]. The new widths are more narrow, but by amounts too small to change the number and/or indices of the

theory shown in table 4 will very likely be removed if the effects of the various experimental parameters are included in an appropriate manner. If this is the case, the QB spectra presented here should be the most accurate data available. This also suggests that the potential function presented here is not questioned by the experimental data [1–3] and that the potential suggested by the fit of these data to spectroscopic formulae [5] will not represent an improvement.

Acknowledgement

References

[1] J. Schopman and J. Los, Physica 48 (1970) 190.

[2] J.C. Houver, J. Baudon, M. Abignoli, M. Barat, P. Fournier and J. Durup, Internat. J. Mass. Spectrom. Ion Phys. 4 (1970) 137.

[3] J. Schopman, P.G. Fournier and J. Los, Physica 63 (1973) 518.

[4] J.M. Peek, Physica 64 (1973) 93.

[5] R.B. Bernstein, Chem. Phys. Letters 25 (1974) 1.

[6] W. Kołos, Internat. J. Quantum Chem. (in publication).

[7] L. Wolniewicz, J. Chem. Phys. 43 (1965) 1087.

[8] S. Peyerimhoff, J. Chem. Phys. 43 (1965) 998.

[9] T.A. Green, H.H. Michels, J.C. Browne and M.M. Madsen, J. Chem. Phys. 61 (1974) 5186.

[10] R.J. LeRoy and R.B. Bernstein, J. Chem. Phys. 54 (1971) 5114.

[11] J.M. Peek, unpublished.

[12] J.G. Maas, N.P.F.B. van Asselt and J. Los, Chem. Phys. 8 (1975) 37.

[13] J.M. Peek, J.G. Maas and J. Los, Chem. Phys. 8 (1975) 46.